

## ION ENGINE PLUME INTERACTION CALCULATIONS FOR PROTOTYPICAL PROMETHEUS 1

M. J. Mandell, (858) 826-1622, Myron.J.Mandell@saic.com

R. A. Kuharski, (858) 826-1621, Robert.A.Kuharski@saic.com

B. M. Gardner, (858) 826-1614, Barbara.M.Gardner@saic.com

Science Applications International Corporation

10260 Campus Point Drive, San Diego, CA 92121 (Fax 858-826-6584)

I. Katz, T. Randolph, R. Dougherty

Jet Propulsion Laboratory

D. C. Ferguson

NASA/Marshall Space Flight Center

### Abstract

Prometheus 1 is a conceptual mission to demonstrate the use of atomic energy for distant space missions. The hypothetical spacecraft design considered in this paper calls for multiple ion thrusters, each with considerably higher beam energy and beam current than have previously flown in space. The engineering challenges posed by such powerful thrusters relate not only to the thrusters themselves, but also to designing the spacecraft to avoid potentially deleterious effects of the thruster plumes. Accommodation of these thrusters requires good prediction of the highest angle portions of the main beam, as well as knowledge of elastically scattered and charge exchange ions, predictions for grid erosion and contamination of surfaces by eroded grid material, and effects of the plasma plume on radio transmissions. Nonlinear interactions of multiple thrusters are also of concern.

In this paper we describe two- and three-dimensional calculations for plume structure and effects of conceptual Prometheus 1 ion engines. Many of the techniques used have been validated by application to ground test data for the NSTAR and NEXT ion engines. Predictions for plume structure and possible sputtering and contamination effects will be presented.

### Introduction

Prometheus 1 is a conceptual mission to develop and demonstrate the ability to use atomic energy to fuel missions to distant destinations. Propulsion would be provided by clusters of large ion engines, powered by a nuclear fission reactor. There are many engineering challenges to designing this extraordinary space vehicle. In this paper we describe our techniques for characterizing the ion engine plumes, particularly at large angles relative to the thrust axis, so that the spacecraft design can accommodate potential sputtering and contamination hazards caused by these plumes.

### Background

Ion engines are a proven space technology. At least 84 Boeing XIPS thrusters, in 13 cm and 25 cm sizes, have flown on at least 21 satellites, clocking over 68,000 hours in space. NASA's 30 cm NSTAR engine completed a mission of over 16,000 hours on the DS1 spacecraft (Figure 1), and has been studied under laboratory conditions for a long-term endurance test of over 30,000 hours.

Figure 2 shows schematically the operation of an ion engine. The "Discharge Chamber" contains plasma maintained at high positive potential. The "Discharge Hollow Cathode" provides electrons that are trapped by a static magnetic field and ionize the working gas (usually Xenon). The "Ion Extraction Grids" (shown here as flat, but usually dished for space applications) form "beamlets" of high energy ions. The inner "screen" grid is maintained at the high positive potential of the discharge chamber, while the outer "accel" grid is maintained a few hundred volts negative to prevent electron backstreaming. The holes in the "screen" and "accel" grids are aligned, so that the plasma emerges from the engine as a set of beamlets that rapidly merge. Finally, the "Neutralizer Hollow Cathode" provides electrons that assure the charge and current neutrality of the ion beam.

Much of this paper focuses on formation of beamlets by the “Ion Extraction Grids” or “Ion Optics.” Extraction is performed by electric fields that penetrate into the discharge chamber plasma from the grid gap region. The shape of the associated potential contours, as well as the amount of current in the beamlet, is determined by the local plasma density near the screen grid. This plasma density commonly varies by a factor of two or more from the center of the ion optics to the outer portions. If the field penetration is large, most ions will have a substantial radial component of velocity as they pass through the screen grid. For high current beamlets ion space charge plays a substantial role in focusing ions in the axial direction, but the space charge focusing is less effective in low current beamlets.

Table 1 shows the progression from the well-studied NSTAR engine toward the conceptual ‘Herakles’ ion engine to be designed for Prometheus 1. Herakles design would be based on the advanced features developed in the HiPEP<sup>1</sup> and NEXIS<sup>2</sup> programs.

The main concerns for spacecraft accommodation of the ion engine plumes are sputtering of surfaces by the energetic ions in the plume and contamination of surfaces by material sputtered from the ion optics grids or from other surfaces. Distortion of electromagnetic signals passing through the plume is also of concern.

Computational tools used in this work include:

- The CEX2D<sup>3</sup> ion optics code provided by NASA/JPL, which is used to calculate the ion beamlet angular distribution. These results are then used to derive the angular distribution for the entire beam.
- EPIC<sup>4, 5</sup> (Electric Propulsion Interactions Code) which is maintained by the NASA/SEE Program and SAIC. EPIC calculates the 3-D interaction of plumes with spacecraft.
- PlumeTool, which is a part of EPIC, is used to calculate plume expansion of the main beam, the elastically scattered ion distribution, and the charge exchange ion plume.

The techniques used in this paper have been validated against laboratory data for the NSTAR<sup>6</sup> and NEXT<sup>7</sup> engines, and the results presented here are for the larger NEXIS engine, using current design parameters for the accel and screen grid thicknesses, hole diameters, and separation.

### Beamlet Divergence and Main Beam Angular Distribution

We use the CEX2D code to calculate the angular distribution of beamlets for the expected range of beamlet currents. CEX2D tracks ion trajectories in axisymmetric geometry self-consistently with their contributions to ion space charge. From the trajectory exit angle (downstream from the accel grid) as a function of the trajectory’s initial radius (upstream of the screen grid) we can calculate the angular distribution of ions in the beamlet.

Figure 3 shows CEX2D tracer trajectories for a high-current NEXIS beamlet. The ions are accelerated radially inward as they enter the ion optics region, and most are then repelled from the axis by the ion space charge. However, ions that enter near the circumference of the screen grid hole have sufficient radial velocity to pass through the space charge region and exit the optics region at high angle. In the case shown, the highest angle trajectory exits at about ten degrees from the axial direction.

Figure 4 shows CEX2D tracer trajectories for a low-current NEXIS beamlet. The extraction fields penetrate farther into the discharge chamber plasma, leading to increased radial acceleration for the outer trajectories. No space charge focusing is apparent. The inset shows the angular current distribution for a low-current beamlet. The distribution is well-fit by an exponential and has a sharp cutoff at about 30 degrees.

To calculate the flux at a field point in the thruster plume, it is necessary to integrate over the entire thruster surface, taking into account the current density, dishing angle, and beamlet angular distribution at each source point. For field points within a few meters of the thruster there will be a distribution of ion velocity directions, and the ion flux cannot be well-fit by a simple model or description. For field points distant from the thruster, main beam ions will be present to a maximum angle of 45 degrees: 15 degrees due to dishing of the grid plus 30 degrees due to divergence of the low-current outer beamlets. Figure 5 shows the cumulative angular distribution for NEXIS at large distances. Although 90% of the beam lies within twenty degrees of the thruster axis, the remaining 10% is distributed to angles as large as 45 degrees.

### Plume Components

An ion engine thruster plume can be thought of as consisting of three components: the high energy main beam ions, low energy charge exchange ions, and intermediate energy elastically scattered ions. The sources of these components are respectively: ionization in the thruster (main beam), charge-exchange downstream of the thruster exit, and elastic scattering with neutral particles also downstream of the thruster exit.

In the computation of the main beam densities and fluxes, the plume is assumed to be a collisionless, singly-ionized, quasi-neutral plasma expanding under the influence of the (density-gradient) electric field. A self-consistent Lagrangian approach is used.

Charge exchange scattering is a process by which fast ions from the main beam undergo charge-exchange with neutral particles, resulting in slow-moving ions and fast-moving neutrals. The charge exchange rate is given by the product of the main beam ion densities and the neutral gas density. The charge-exchange density and flux are computed using a particle-in-cell (PIC) algorithm.

The third ion component computed by the plume model is due to these elastic scattering events that occur between main beam ions and stationary neutrals. Elastically scattered high energy ions can dominate the main beam ions at large angles (greater than about 45°) and may thus pose serious spacecraft integration concerns. The computation assumes that the scattered ions travel in straight lines. The density and flux at each location are computed by numerically integrating over all source locations.

Figure 6 shows contours of the two-dimensional plume density, including all three components. The low energy charge exchange component extends to angles beyond 90 degrees.

### Sputtering of Carbon from Accel Grid

An important source of contamination is sputtering of the Carbon-Carbon accel grid by charge exchange ions. These ions are accelerated to energies of 500 eV by the electron-repelling potential applied to the grid. Sputtering of these carbon materials was studied by Williams *et al.*<sup>8</sup> The sputter products are not distributed in a simple cosine pattern, but rather in a “butterfly” pattern that gives substantial sputtered flux at high angles. By integrating over the engine surface and calculating the flux sputtered from each source point toward the desired field point (code similar to that used to calculate the main beam flux) we can calculate the carbon flux from the thruster to any field point. Results (Figure 7) show substantial sideways flux, with carbon fluxes extending to 105 degrees from the thruster axis.

### Summary

We have demonstrated tools and techniques to calculate plume densities and fluxes from large ion thrusters. The results were validated by comparison with laboratory data on the NSTAR, NEXT, and NEXIS thrusters, and by NSTAR space data.

For large thrusters we would expect to see energetic main beam ions up to 45 degrees from the plume axis. In our analyses, charge exchange ions and sputtered carbon are found beyond 90 degrees from the plume axis.

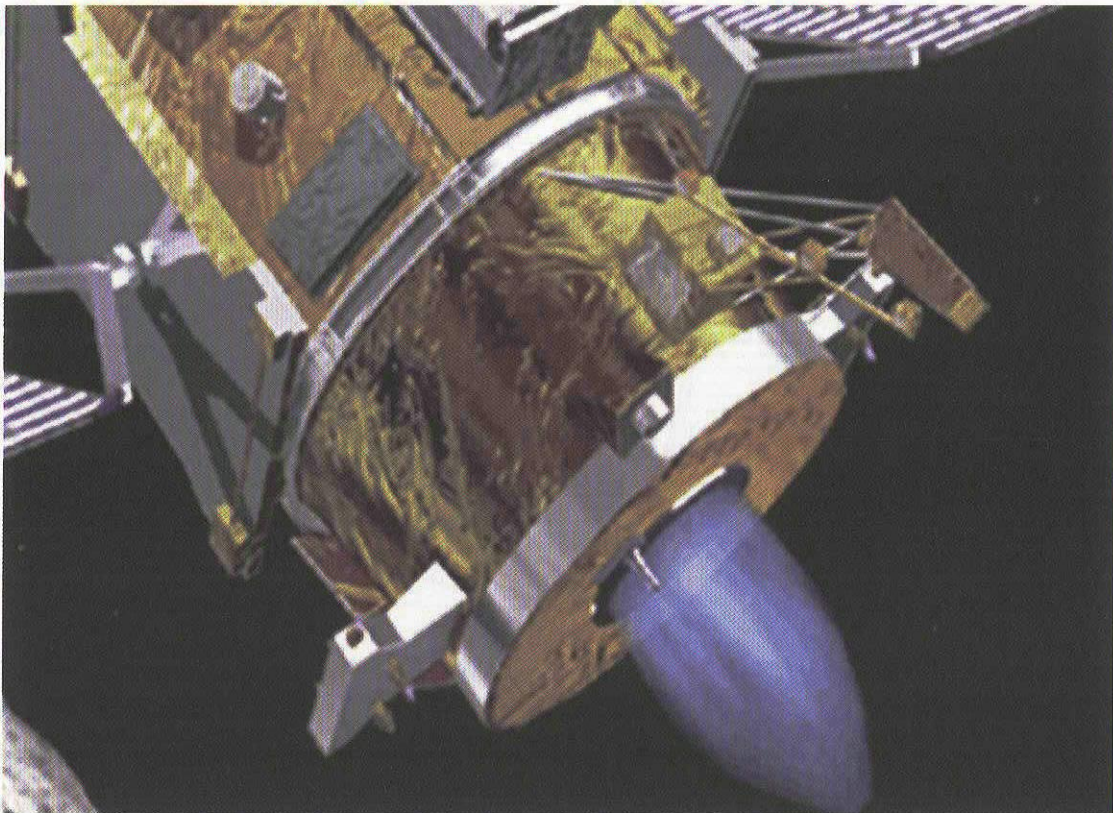
Future plans include modeling the Herakles thruster plume when design details become available and modeling multiple plume interactions using *Nascap-2k*.<sup>9</sup>

### Acknowledgements

The work summarized in this paper was funded by the Prometheus 1 Mission Assurance office, and by the Space Environment Effects Program at the Marshall Space Flight Center under contact number NNM04AB37C. The authors wish to thank Billy Kauffman of MSFC for his support over the years.

**Table 1.** Progression of large ion engines from NSTAR to HERAKLES.

	NSTAR	NEXT	HIPEP	NEXIS	HERAKLES
<b>Diameter (cm)</b>	30	40	(rectangular)	65	>80
<b>Beam Energy (eV)</b>	1100	1800	3650	3700	TBD
<b>Current (A)</b>	1.8	3.52	6.15	4.57	TBD
<b>Mean Current Density (Am<sup>-2</sup>)</b>	28.8	34.1	16.4	17.6	TBD
<b>Specific Impulse (s)</b>	3170	4100	6000-9000	>6000	6000-8000
<b>Grid Material</b>	Mo	Mo	Pyro. Graphite	C-C	TBD

**Figure 1.** The NSTAR thruster completed a mission of over 16,000 hours as part of the DS1 spacecraft.

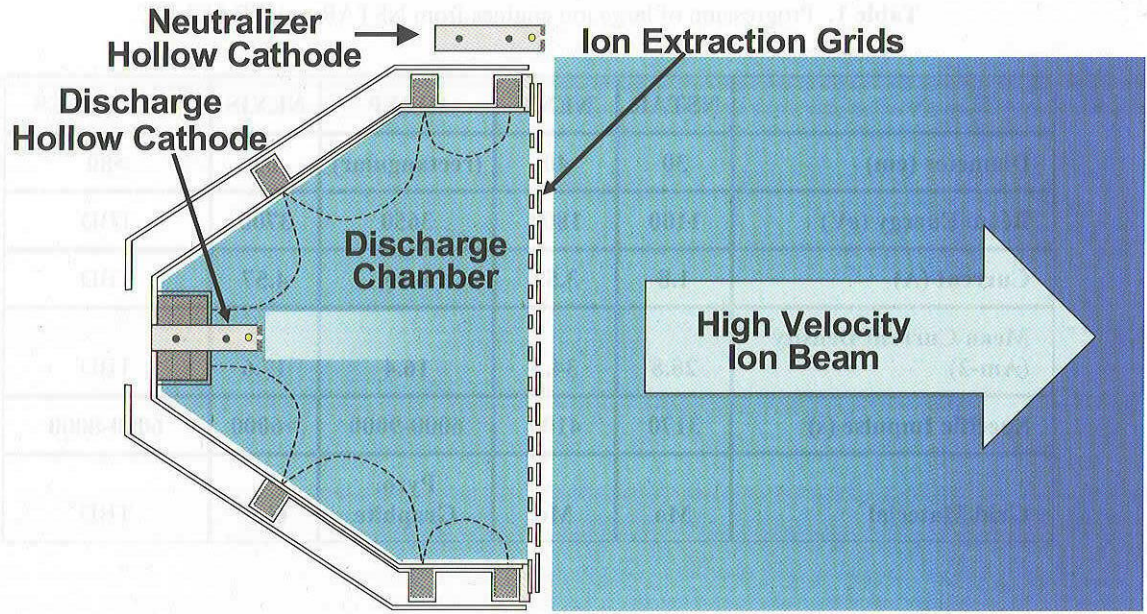


Figure 2. Basic operation of an ion engine. Note that the “Ion Extraction Grids,” which consist of the screen and accel grids, and which are shown here as flat, are usually dished for space operation.

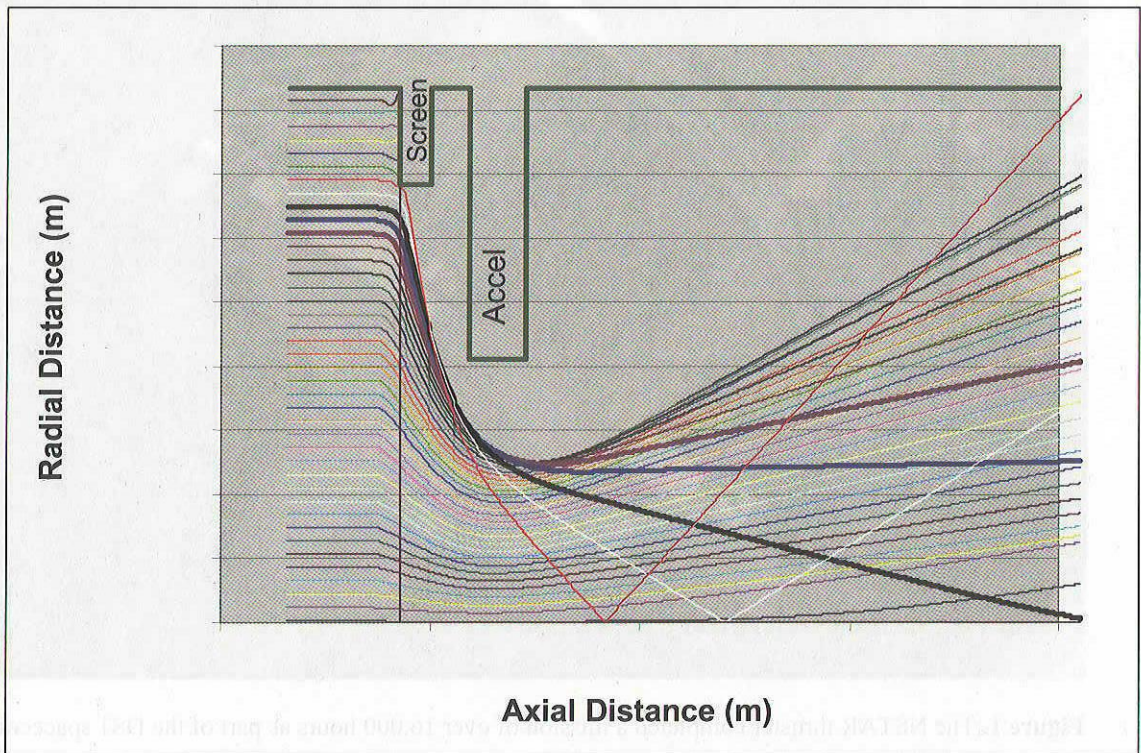
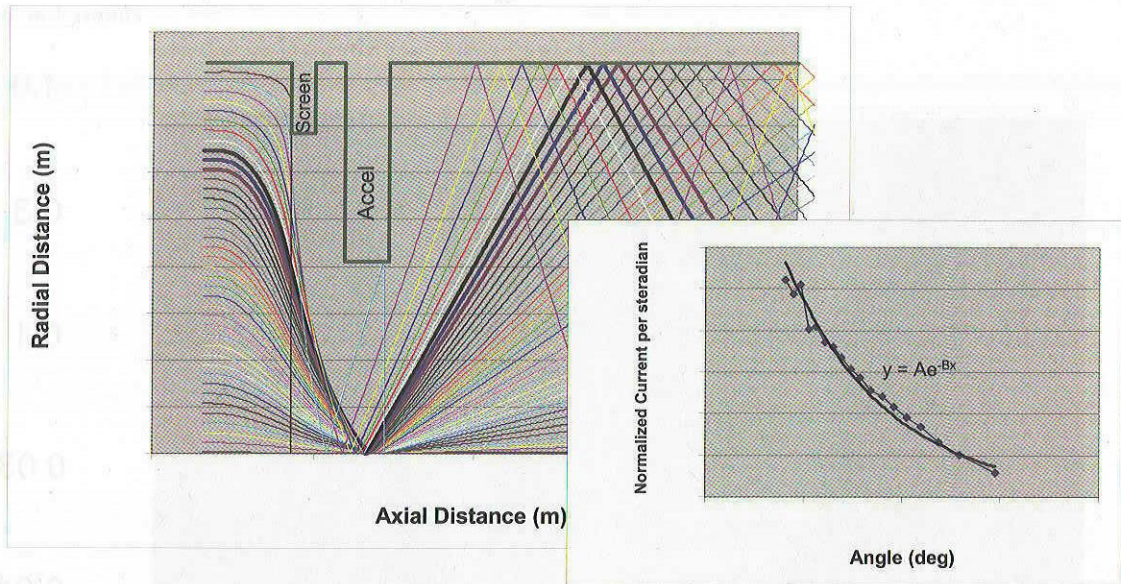
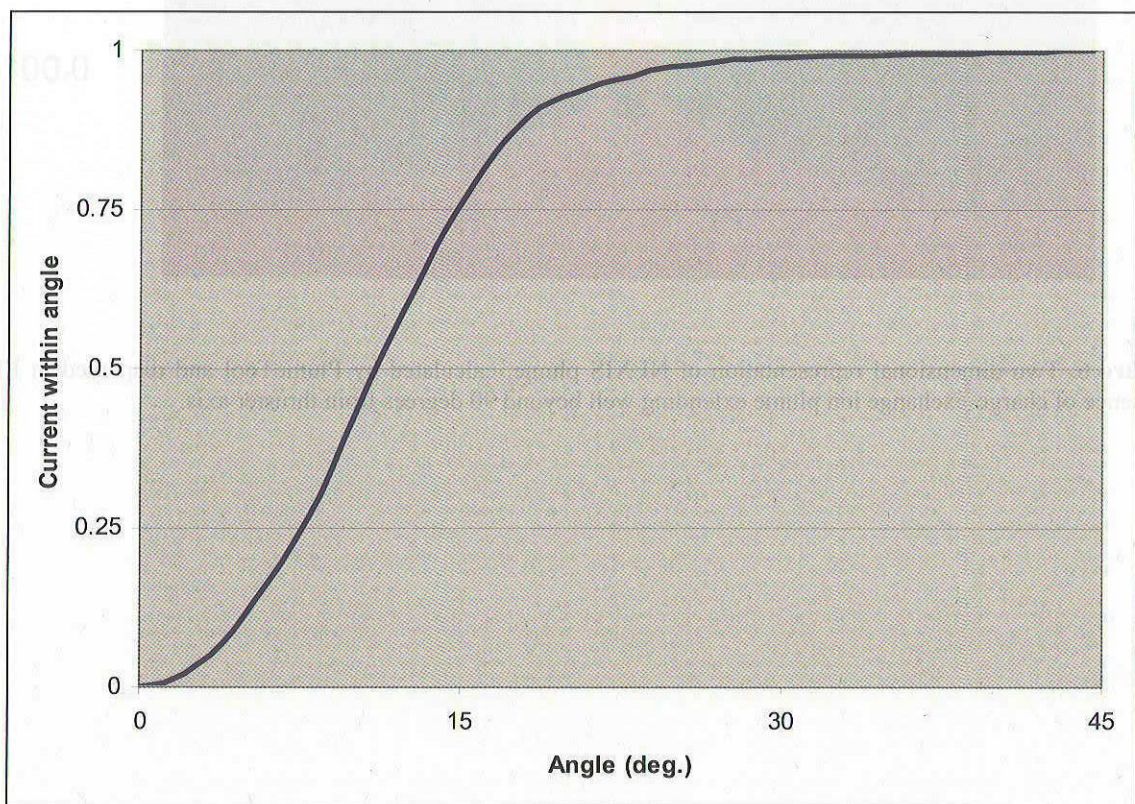


Figure 3. CEX2D-calculated ion trajectories for a high-current NEXIS beamlet. The highest angle trajectory is seen to bounce off (cross) the axis and exit at an angle of about ten degrees.



**Figure 4.** CEX2D-calculated ion trajectories for a low-current NEXIS beamlet. Numerous trajectories bounce off the axis and exit at angles up to 30 degrees. The inset shows the angular distribution for a low-current beamlet, which is well-fit by an exponential form.



**Figure 5.** Cumulative angular distribution of NEXIS main beam ions at large distances.

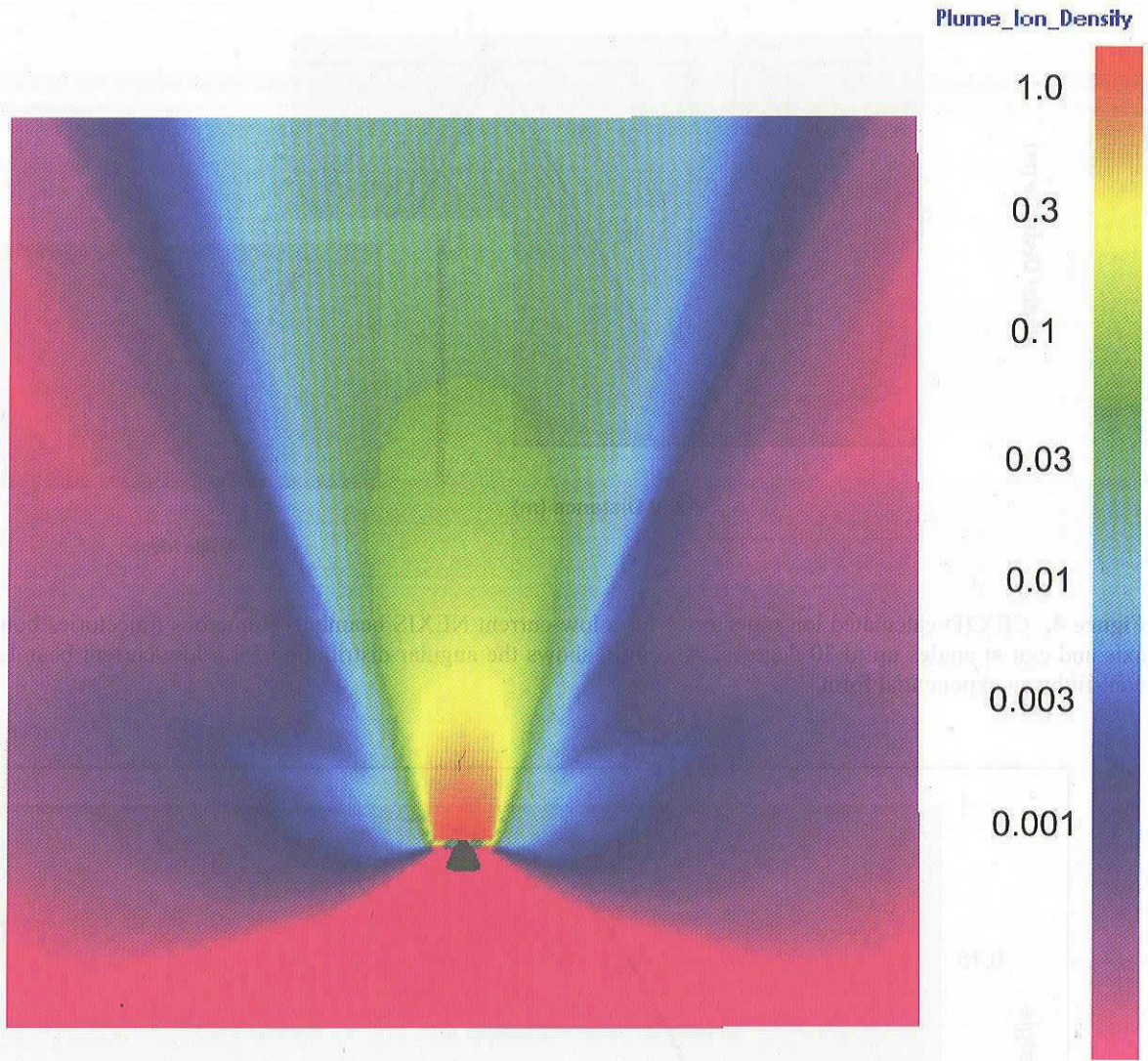


**Figure 6.** Two-dimensional representation of NEXIS plume, calculated by PlumeTool and displayed in EPIC. Note presence of charge-exchange ion plume extending well beyond 90 degrees from thruster axis.

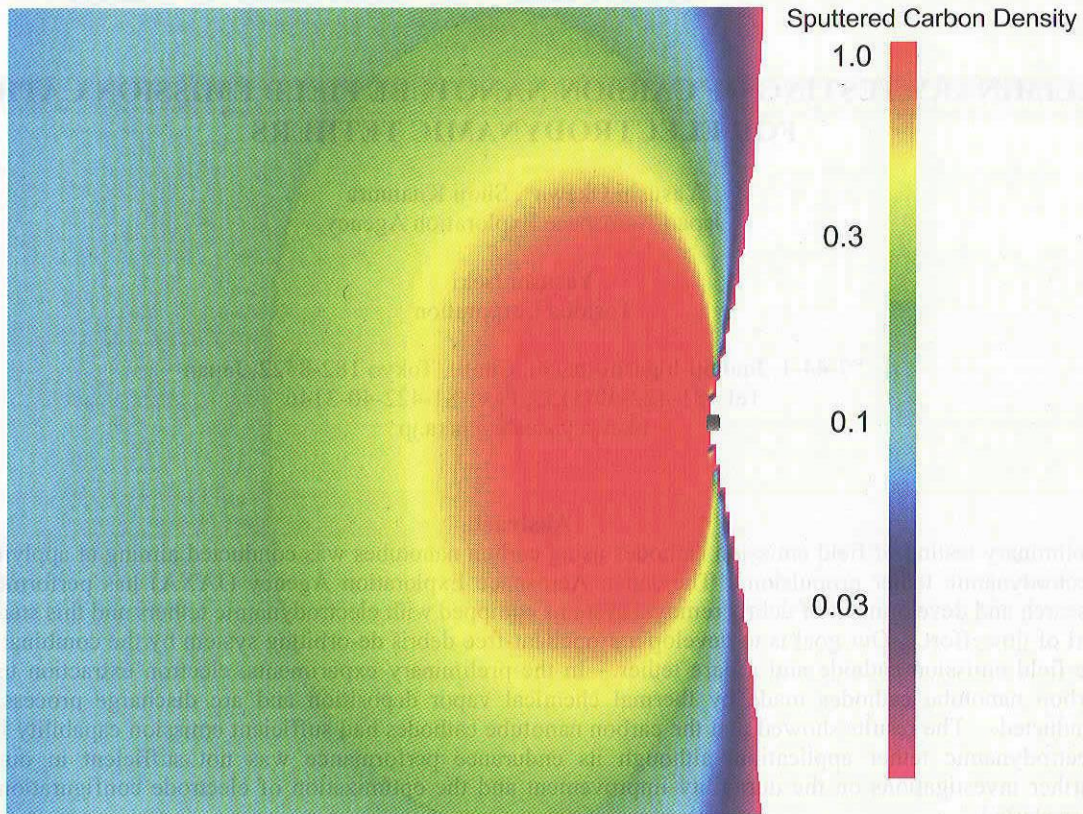


**Figure 7.** Density distribution of carbon sputtered from the accel grid.

## References

- <sup>1</sup> Elliott, F. W., J. E. Foster, M. J. Patterson, "An Overview of the High Power Electric Propulsion (HiPEP) Project," AIAA-2004-3453, 2004.
- <sup>2</sup> Randolph, T. M., and J. E. Polk, "An Overview of the Nuclear Electric Xenon Ion System (NEXIS) Activity," AIAA-2004-3450, 2004.
- <sup>3</sup> Brophy, J. R., I. Katz, J. E. Polk, J. R. Anderson, "Numerical Simulations of Ion Thruster Accelerator Grid Erosion," AIAA-2002-4261, 2002.
- <sup>4</sup> Mikellides, I. G., Kuharski, R. A., Mandell, M. J., Gardner, B. M., "Assessment of Spacecraft Systems Integration Using The Electric Propulsion Interactions Code (*EPIC*)," AIAA-2002-3667, 2002.
- <sup>5</sup> EPIC is made available to U. S. citizens by the SEE program at <http://see.msfc.nasa.gov>.
- <sup>6</sup> Sengupta, A., J. R. Brophy, K. D. Goodfellow, "Status of the Extended Life Test of the Deep Space I Flight Spare Ion Engine after 30,352 Hours of Operation," AIAA-2003-4558, 2003.
- <sup>7</sup> Kamhawi, H., G. C. Soulas, M. J. Patterson, M. M. Frandina, "NEXT Ion Engine 2000 hour Wear Test Plume and Erosion Results," AIAA-2004-3792, 2004.
- <sup>8</sup> Williams, J. D., M. L. Johnson, and D. D. Williams, "Differential Sputtering Behavior of Pyrolytic Graphite and Carbon-Carbon Composite Under Xenon Bombardment," 40th AIAA/ASME/SAE/ASEE Joint Propulsion Conference and Exhibit, 11-14 July 2004, Fort Lauderdale, FL.
- <sup>9</sup> Mandell, M. J., V. A. Davis, D. L. Cooke, A. Wheelock, "Nascap-2k Spacecraft Charging Code Overview," 9<sup>th</sup> Spacecraft Charging Technology Conference, Tsukuba, Japan (2005).